Magnetic-resonance study of Mn^{2+} impurity modes in $FeBr_2$

A. R. King
Department of Physics, University of California, Santa Barbara, California 93106

Y. Merle-d'Aubigné
Department of Physics, University of California, Santa Barbara, California 93106
and Laboratoire de Spectrométrie Physique, Boîte Postale 53, Centre de Tri, 38041 Grenoble Cedex, France

S. M. Rezende and E. A. Soares
Department of Physics, University of California, Santa Barbara, California 93106
and Departamento de Física, Universidade Federal de Pernambuco, Recife, Brazil
(Received 2 June 1978)

The spin resonance of Mn^{2+} impurity modes in the layered antiferromagnet $FeBr_2$ was studied in the frequency range 500–700 MHz. The ^{55}Mn NMR signals are found to have large enhancements due to the admixture of electronic spin transitions. Measurements of the frequency spectrum yield accurate values for the hyperfine, nuclear dipole, and nuclear quadrupole interaction parameters for the Mn impurity. The measured temperature dependence of the linewidth of the NMR modes in the range 1.5–3.5 K can be explained by two-magnon scattering of the $FeBr_2$ host.

I. INTRODUCTION

The study of phenomena associated with impurity spins in magnetically ordered materials has been of considerable interest for some time. Many studies have been made,[1,2] both theoretically and experimentally, of both the frequencies of impurity-associated modes, and the thermodynamic properties associated with their excitations. Recently, there has been renewed interest in the ferrous halides $FeCl_2$ and $FeBr_2$ as a result of several interesting features in their magnetic properties. Among these are the two-dimensional character of their magnetic excitations as revealed by neutron scattering experiments of Yelon and Vettier (YV),[3] and the metamagnetic transition as studied by magnetization[4] and resonance[5] measurements. Recent EPR experiments of Mischler *et al.* (MCM)[6] on Mn^{2+} doped into $FeBr_2$ have shown the unusual result that all the $2S+1$ Mn impurity modes lie well below the bottom of the host band in the low-microwave region, and are hence accessible for study.

In this paper we present the results of NMR studies of Mn^{2+} impurities in antiferromagnetic $FeBr_2$. We are aware of only one other experiment[7] in which the NMR of a magnetic impurity nucleus has been observed in the ordered state of an insulating magnetic material. That case is the Mn^{2+} impurity in $CoCl_2 \cdot 2H_2O$, in which the Mn^{2+} impurity electronic modes also lie in the low-microwave region.[8,9] Some of the effects seen in the present experiment have also been observed in the former one. The present experiments were done in the frequency range 500–700 MHz. In this frequency range, where normally one would expect to find only the ^{55}Mn NMR spectra, we observed the existence of mixed electronic-nuclear transitions due to the low-frequency nature of several of the nominally pure EPR lines. Frequency versus field measurements yield accurate values for the hyperfine, nuclear dipole, and nuclear quadrupole interaction constants for the ^{55}Mn ion in the $FeBr_2$ lattice. The temperature dependence of the linewidth data yields information on the low-k magnons of $FeBr_2$ which, according to our model, relax the nuclear excitations by two-magnon scattering processes.

II. EXPERIMENTS

The experiments were performed using a broadband NMR spectrometer in the frequency range 500–700 MHz between 1.2 and 3.6 K in magnetic fields up to 20 kOe. The NMR spectrometer, developed by one of us (A.R.K.), is a broadband homodyne bridge spectrometer with coherent detection, employing connectorized miniature power dividers, mixer, and amplifier which operate over the whole frequency range 10–1000 MHz. It can be used both for cw and pulsed modes with the sample mounted in broadband untuned or in tuned coils. The experiments reported here were performed in a coil-air capacitor resonator with $Q \simeq 2000$ at low temperature, which could be tuned over the 500–700 MHz range. The sample was grown in Saclay using a Bridgeman technique, and contained 0.3 mole% of Mn^{2+}. The sample and resonator were held out of the liquid in a closed tube filled with He exchange gas, which was immersed in a Dewar of pumped helium. Temperature measurement and control

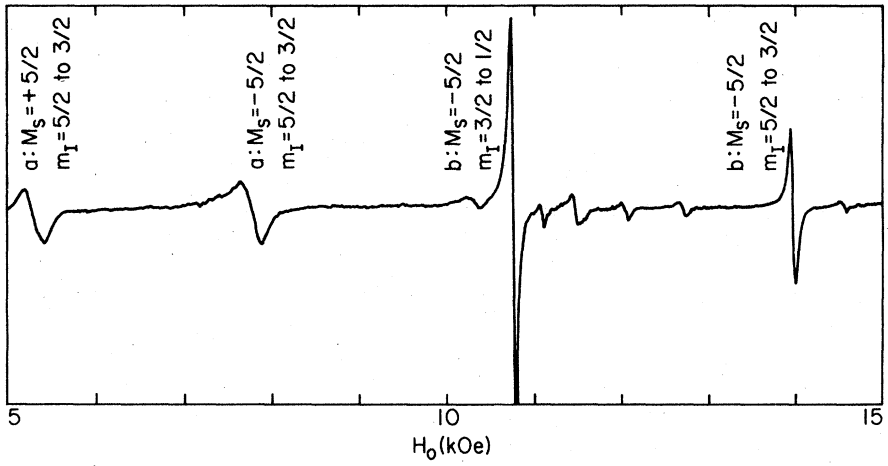

FIG. 1. Typical spectrum at $f = 574$ MHz, $T = 2.4$ K. The four strong transitions are identified, but the origin of the weaker lines is not understood. The two b-sublattice lines show essentially their zero-temperature linewidths, while the two a-sublattice lines show considerable broadening at this temperature.

were accomplished via the He vapor pressure. A typical spectrum is shown in Fig. 1.

III. COUPLED ELECTRONIC-NUCLEAR Mn MODES

The Fe^{2+} spins in $FeBr_2$ ($T_N = 14$ K) were found by YV to have a strong ferromagnetic interaction within hexagonal layers perpendicular to the c axis, and to be subject to large single-ion anisotropy fields which confine them along the symmetry axis. The interplane interaction is antiferromagnetic and is weak, such that the spin waves have essentially two-dimensional ferromagnetic character in the two weakly coupled sublattices. The behavior of the electronic spin of substitutional Mn^{2+} impurities in this system has been recently investigated in detail by MCM who showed that the inter and intraplane Mn-Fe exchange interactions tend to cancel each other. As a result, the Mn^{2+} spin transitions have energies <0.5 cm^{-1} which are much smaller than the host magnon energies >17 cm^{-1}. In the language of the local impurity mode problem, it is found that all $2S$ successive multiple excitations of the defect mode levels lie at very low microwave frequencies.

Since the Ising states of the impurity and host levels are not eigenstates of the Hamiltonian, the local model theories predict that successive excitations of the defect may have unequal spacings, and that impurity levels are not states of pure M_S, an effect entirely analogous to the zero-point deviation observed in pure antiferromagnets.

The above effect is the cause of some of the large and unusual terms in the effective Hamiltonian used by MCM, which can be written as

$$\mathcal{H}_s = g_{\parallel}\mu_B(H_0 + \epsilon H_{\text{int}})S_z + D[S_z^2 - \tfrac{1}{3}S(S+1)] + \epsilon C S_z^3 + \tfrac{1}{60}B(35S_z^4 - 237.5S_z^2 + 177.19), \quad (1)$$

where μ_B is the Bohr magneton, H_0 is the external field applied along the c axis, $S = \frac{5}{2}$, and ϵ takes the values +1 and −1 on alternate sublattices. For convenience, we label the sublattices a and b, respectively. The values of the parameters in Eq. (1) are

$$g_{\parallel} = 1.94, \quad H_{\text{int}} = 2.90 \text{ kOe},$$
$$D/g_{\parallel}\mu_B = -0.77 \text{ kOe}, \quad C/g_{\parallel}\mu_B = -0.07 \text{ kOe}, \quad (2)$$
$$B/g_{\parallel}\mu_B = 0.015 \text{ kOe}.$$

According to the Hamiltonian of Eq. (1), the EPR spectrum of the impurity consists of two groups of five lines each, some with frequency increasing with increasing field and others with frequency decreasing with field. In the latter, crossings occur between nuclear and electronic levels, giving rise to admixtures of the electronic- and nuclear-spin transitions. In order to describe these mixed excitations, we consider the Hamiltonian for the nuclear spins

$$\mathcal{H}_I = \gamma_n\hbar[H_0 + \epsilon(H_d + H_{\text{ST}})] + \hbar Q[I_z^2 - \tfrac{1}{3}I(I+1)], \quad (3)$$

and for the hyperfine coupling

$$\mathcal{H}_{\text{hf}} = \hbar A(S_z I_z + \tfrac{1}{2}S_+ I_- + \tfrac{1}{2}S_- I_+). \quad (4)$$

Here γ_n is the nuclear gyromagnetic ratio, $I = \frac{5}{2}$, Q is the nuclear quadrupole constant, and H_d is the dipolar field created on the Mn nuclei by the host Fe^{2+} spins. A is the impurity hyperfine interaction constant and H_{ST} is the supertransferred hyperfine field[10] on the Mn nucleus due to host electronic spins.

The nature of the NMR spectrum due to Eqs. (1), (3), and (4) depends in detail on the time dependence of the impurity electronic-spin motion, and, in particular, on the characteristic time τ_c for the decay of the autocorrelation function of S_z. We discuss two limiting cases, in which considerably different behaviors of the NMR spectrum are observed.

In the limit $\tau_c \ll 1/A$, the dephasing of a nuclear spin during τ_c is much less than 1 rad, and the electronic-spin samples all occupied levels many times during a single nuclear Larmor period. The NMR shows a single temperature-dependent frequency $\omega_n \sim A\langle S_z\rangle$, where $\langle S_z\rangle$ is the thermal average over the states of S_z. This is the familiar case of NMR in exchange-coupled magnetic materials studied by Hone, Callen, and Walker,[11] where $1/\tau_c \sim \omega_E$, the exchange frequency. Typically, $\tau_c \sim 1/\omega_E \ll 1/A$, giving an exchange-narrowed linewidth $\Delta\omega_n \sim A^2/\omega_E$. The impurity mode, if not degenerate with host modes, need not have a short τ_c, and in fact τ_c is determined not by exchange, but by the available relaxation processes for both T_1 and T_2. These rates were fast enough for all the impurities studied in MnF_2,[12] that the impurity-associated ^{19}F NMR did indeed measure $\langle S_z\rangle$. These systems all had the local impurity modes lying either above the top of the host band or, in the case of Zn impurities, of the modes of the Mn neighbors of the Zn lying withing the band. They might therefore be expected to have stronger relaxation processes than the present case of modes well below the host band.

If, however, $\tau_c \gg 1/A$, the nucleus precesses through many Larmor periods within τ_c, so NMR is done in a discrete level of S_z. The NMR frequency does *not* reflect $\langle S_z\rangle$; but rather a series of frequencies corresponding to the discrete values of S_z, i.e., temperature-independent resonant frequencies $\omega_n \approx AM_s$. The intensities of the individual resonances reflect the populations of the corresponding electronic levels, giving the first moment of the NMR spectrum $\langle\omega_n\rangle \propto A\langle S_z\rangle$, with the temperature dependence occurring in the intensities, not the frequencies. Since the local modes are not exact eigenfunctions of S_z, the NMR is in principle capable of measuring the zero-point deviation in each impurity level. The Mn NMR in $FeBr_2$ is seen to be an example of this limit, since temperature-independent NMR frequencies corresponding to both $M_s = \pm\frac{5}{2}$ spin levels on both sublattices were observed. NMR spectra due to the levels $M_s = \pm\frac{3}{2}, \pm\frac{1}{2}$, would be expected at frequencies roughly $\frac{3}{5}$ and $\frac{1}{5}$ of those observed, but were below tuning range of the resonant circuit used. The diagonal parts of Eqs. (3) and (4) give nuclear transitions $\Delta m_I = \pm 1, \Delta M_s = 0$, with frequencies

$$\omega_{m_I \to m_I - 1} = -\gamma_n[H_0 + \epsilon(H_d + H_{ST})] + AM_s + Q(2m_I - 1)\,. \tag{5}$$

The dominant term in Eq. (5) is AM_s, which for $M_s = \pm\frac{5}{2}$ is approximately 600 MHz. This is, however, a very poor approximation to the frequency, due to the proximity of the low-lying electronic modes.

In order to calculate exactly all the transition frequencies of the system, one must diagonalize the total Hamiltonian, for which the eigenstates of S_z and I_z can be used as a basis. However, since our measurements were made only in the frequency range close to the NMR transition corresponding to $M_s = \pm\frac{5}{2}$, we have carried out the diagonalization approximately within the subspace of $|M_s, m_I\rangle$ and $|M_s \pm 1, m_I \mp 1\rangle$, where $M_s = \pm\frac{5}{2}$. This procedure is equivalent to second-order perturbation theory. The results of the calculation explain very well the measured field dependence of the frequency spectrum, as demonstrated in Fig. 2. The fitting of the data to the calculation yielded the following parameters for the nuclear-spin Hamiltonian of the ^{55}Mn impurity.

$$\begin{aligned} &\gamma_N/2\pi = 1.05 \text{ MHz/kOe}, \quad AS/2\pi = -579 \text{ MHz}\,, \\ &Q/2\pi = 0.225 \text{ MHz}, \quad H_d + H_{ST} = 3.31 \text{ kOe}\,. \end{aligned} \tag{6}$$

Note that since both $M_s = \pm\frac{5}{2}$ levels are observed, the contributions to ω_n from the impurities' own electronic spin may be separated from those due to host spins, unlike the case of the pure materials. Since A is affected by covalency we attempted to estimate the zero-point spin deviation by comparing our measured value with that obtained by EPR of Mn^{2+} in $CsMgBr_3$,[13] in which the Mn site is also octahedrally coordinated by Br^- ions. Those results give the same values of A as ours, but with accuracy sufficient to conclude only that the zero-point deviation is less than 3%. The value of H_{ST} cannot be uniquely derived by subtracting the calculated value of $H_d = 8.0$ kOe from the measured $(H_d + H_{ST})$. The sign of H_d is not known, since the identification of the a and b spectra with sublattice magnetization has not been made. The two possible values of H_{ST} are +11.31 and −4.69 kOe.

Notice that a typical spectrum in the frequency range of Fig. 2 has actually more lines than are shown; these were left out of the figure for the sake of clarity. The four groups of lines—a, $M_s = \pm\frac{5}{2}$ and b, $M_s = \pm\frac{5}{2}$—correspond to transitions with $\Delta m_I = \pm 1$ far from the level-crossing region. Thus, even though they are strongly coupled to electronic transitions, they have slopes of the order of 1 MHz/kOe, the value of γ_n, and may be properly called NMR lines. On the other hand, lines with slopes of the order of a few GHz/kOe correspond to essentially pure electronic transitions, such as the two shown in the figure.

One of the most interesting features of the observed spectra is the large intensity of some of the NMR lines, particularly in view of the fact that the impurity concentration is small. These large intensities result from an enhancement of the nuclear

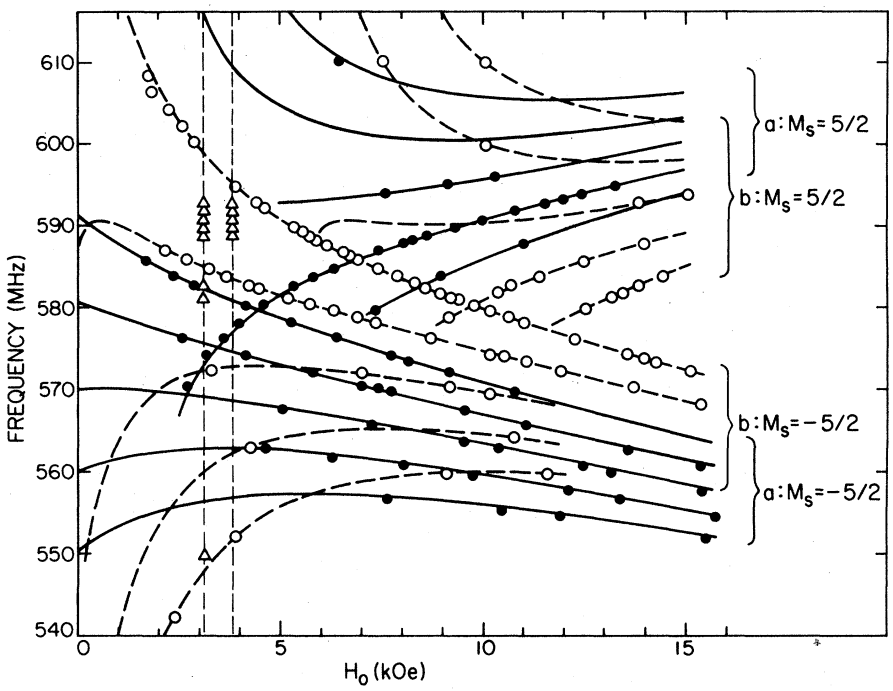

FIG. 2. NMR frequency spectrum of the $M_s = \pm\frac{5}{2}$ levels of ^{55}Mn in $FeBr_2$. Solid lines and solid circles correspond to the a sublattice; dashed lines and open circles correspond to the b sublattice. The lines represent Eqs. (5) and (6); the points are experimental. The two vertical dashed lines and the triangular points are the EPR transitions on the b sublattice $M_s = \frac{1}{2} \longleftrightarrow -\frac{1}{2}$ and $M_s = \frac{3}{2} \longleftrightarrow \frac{1}{2}$.

transitions by the admixture of electronic excitation. Consider the states corresponding to two energy levels which undergo transitions with $\Delta m_I = \pm 1$

$$|\psi^m\rangle = a_m |M_s, m_I\rangle + b_m |M_s - 1, m_I + 1\rangle ,$$
$$|\psi^{m-1}\rangle = a_{m-1} |M_s, m_I - 1\rangle + b_{m-1} |M_s - 1, m_I\rangle . \quad (7)$$

Far from the level crossing, these coefficients are approximately $a_m \simeq a_{m-1} \simeq 1$ and $b_m \simeq b_{m-1} \simeq A/2\omega_e(M_s, M_s - 1)$, where $\omega_e(M_s, M_s - 1)$ is the essentially pure electronic-transition frequency. We now assume that the system is driven by an rf field H_1 which couples to both nuclear and electronic spins. In spite of the fact that the electronic admixture in the states Eq. (7) is small, its coupling to the driving field is γ_e/γ_n larger than the coupling of the nuclear spins. As a result the intensity of the absorption of the transition $|\psi^m\rangle \longleftrightarrow |\psi^{m\pm1}\rangle$ is enhanced with respect to the purely nuclear transition $|M_s, m_I\rangle \longleftrightarrow |M_s, m_I \pm 1\rangle$. The enhancement factor in the driving field is, far from the level crossing

$$\eta \simeq \frac{5}{2} \frac{\gamma_e}{\gamma_n} \frac{A}{\omega_e(M_s, M_s \pm 1)} \quad (8)$$

for $M_s = \pm\frac{5}{2}$. This enhancement was noticed by Abragam[14] in connection with electron-nuclear double resonance measurements. A similar effect was very recently observed by Bleaney *et al.*[15] in the singlet ground state of Ho^{2+} in $HoVO_4$.

By measuring cw saturation and the duration of 180° and 90° pulses, we have been able to infer the effective driving field experienced by the nuclear spins. Comparison with the actual fields produced by the coil showed, for example, that the enhancements of the NMR lines corresponding to $M_s = -\frac{5}{2}$, for both sublattices, were as large as about 100. This is also the value one obtains from Eq. (8). The measurements also demonstrated that the intensities decrease with increasing H_0, clearly a result of the increasing value of the electronic frequency.

IV. LINEWIDTH AND RELAXATION OF THE NMR

The linewidths of several NMR lines were measured as a function of temperature in cw experiments. The longitudinal and transverse relaxation times T_{1n} and T_{2n}, were measured by standard pulse techniques, which required little power because of the enhancements described earlier. The linewidth data for three groups of lines, shown in Fig. 3, exhibit similar features. At low temperatures the lines are inhomogeneously broadened, as evidenced by the development of spin echoes in the pulsed NMR. This broadening is probably a reflection of the inhomogeneous broadening of the EPR, through the "pulling" of the NMR frequency. It is easily shown that the NMR width δH_n is related to the EPR width δH_e by

$$\delta H_n \sim (1 - \gamma_{0n}/\gamma_n)\delta H_e , \quad (9)$$

where γ_n and γ_{0n} are the observed and "bare" nuclear gyromagnetic ratios, respectively. Using

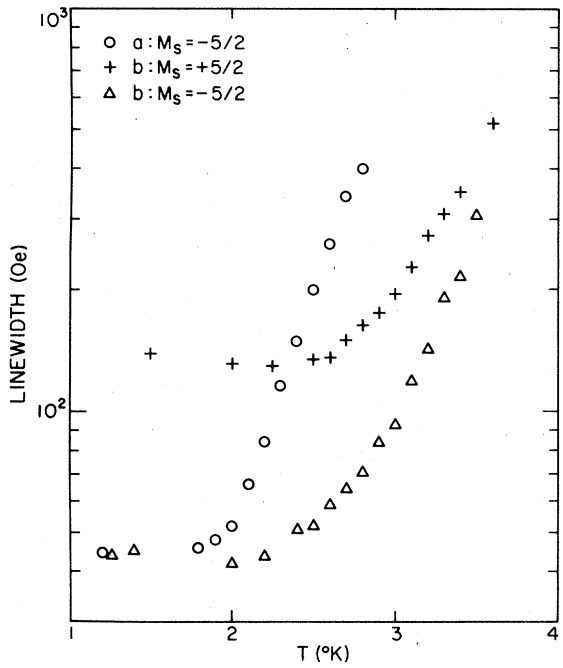

FIG. 3. Linewidth vs temperature for three ^{55}Mn NMR transitions. The points correspond to the following conditions: open circles, a sublattice, $M_s = -\frac{5}{2}$, $f = 565$ MHz, $H_0 = 11.7$ kOe; crosses, b sublattice, $M_s = +\frac{5}{2}$, $f = 583$ MHz, $H_0 = 11.0$ kOe; triangles, b sublattice, $M_s = -\frac{5}{2}$, $f = 574$ MHz, $H_0 = 10.5$ kOe. All nuclear transitions are between the $m_I = +\frac{1}{2}$ and $+\frac{3}{2}$ levels.

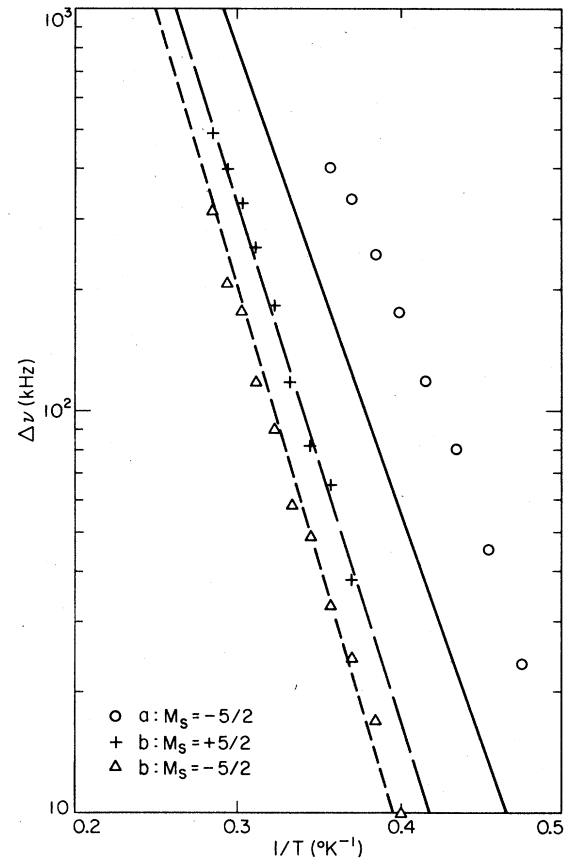

FIG. 4. Temperature-dependent part $\Delta\nu$ of the ^{55}Mn NMR linewidth plotted logarithmically vs $1/T$. The points are the same as those of Fig. 3, and the lines represent the theory of Eq. (14). The two b-sublattice points can be fit simultaneously with the same choice of parameters, but the a-sublattice data lie a factor of 3 higher than the calculation.

values of γ_n calculated from the computer fit to the spectrum and an EPR width $\Delta H_e = 315$ Oe results in a very satisfactory fit to the low-temperature NMR linewidths. This value agrees very well with EPR measurements in similar crystals. As the temperature increases the lines broaden so rapidly that at 4.2 K the spectrum cannot be observed.

Both the high- and low-temperature line shapes are very nearly Lorentzian. This allows us to determine the temperature-dependent part $(1/T_{2n})$ of the linewidth by simply subtracting the low-temperature width from the measured one.

Two features of the linewidth behavior become apparent when its temperature-dependent part is plotted separately (Fig. 4). First, the $1/T_2$ curves join smoothly the $1/T_1$ data, which differ from $1/T_{2n}$ only in the low-temperature half of the range investigated. Second, their temperature dependence is well approximated by $\exp(-\hbar\omega_g/kT)$, where ω_g is the host magnon gap. This immediately suggests that the source of T_{1n} and T_{2n} is a two-magon scattering process proceeding via the hyperfine interaction (Beeman and Pincus[16]). The usual calculation for this process, however, gives relaxation rates several orders of magnitude smaller than the measurements. An alternative model was therefore devised in order to explain the experimental data.

The first ingredient of the model consists of assuming that the Mn nuclear relaxation time T_{2n} is determined by the Mn^{2+} electronic-spin relaxation time T_{1e}. In the limit of long τ_c, the Mn NMR is seen at a given frequency $\sim AM_s$ only while the Mn^{2+} electronic spin is in a well-defined state ($M_s = \pm\frac{5}{2}$). A relaxation process which removes the spin from this M_s level changes the NMR frequency by an amount $\approx A$, removing it from observation. This causes a broadening equal to the inverse lifetime of the state, which is, in turn, equal to the transition rate out of the state. We denote these rates by W_+ and W_- for the $M_s = -\frac{5}{2}$ and $+\frac{5}{2}$ levels, respectively.

Thus the NMR linewidth becomes

$$1/T_{2n} = W_\pm \tag{10}$$

and the problem becomes one of calculating the electronic relaxation rates $W_{\pm}$.

The Mn impurity electronic spin can relax via two-host magon scattering if the impurity-host interaction Hamiltonian contains nondiagonal terms of the type $J^{yz}S_yS_z'$. Here S and S' refer to impurity and host spins, respectively. Expressing the Fe^{2+} spin operators in terms of magnon operators one can show that

$$W_+ = \frac{2\pi}{\hbar^2}\left[S(S+1) - \tfrac{5}{2}\times\tfrac{3}{2}\right]\frac{1}{N^2} \times \sum_{kk'}\left|\sum_{ii'}{}' J^{yz}_{ii'}\sin\tfrac{1}{2}(\vec{k}-\vec{k}')\cdot(\vec{r}_i - \vec{r}_i')\right|^2 \times(\eta_k+1)\eta_{k'}\delta(\omega_k - \omega_{k'} - \omega_e);$$

$$W_- = W_+\exp(-\hbar\omega_e/kT) \tag{11}$$

are the relaxation rates due to a process in which an electronic-spin flip is accompanied by the absorption of a magnon k' and emission of a magnon k. In Eq. (11) ω_e is the transition frequency out of the M_s level, the sum $\sum_{ii'}'$ is over pairs of neighbors placed symmetrically about the impurity within each plane of spins, and η_k is the magnon Bose factor. Since no direct measurements exist on exchange terms of this form, we have used only the dipolar interaction D^{yz}, which is zero between spins on the same sublattice, but would be allowed between the neighbors on each adjacent plane. Although there is a large off-diagonal exchange $J^{xz}S_zS_x'$ which gives rise to the large effective D term in Eq. (1), this term does not contribute to Mn relaxation. It is clear from the calculation by Tachiki[17] that there is no reason for J^{zx} and J^{xz} to be equal. In order to evaluate Eq. (11) analytically we make the following additional assumptions: (a) The sums in k are replaced by integrals. Due to the two-dimensional character of the magnons, one has

$$N^{-1}\sum_k \to \left(\frac{a}{2\pi}\right)^2\int dk^2 .$$

(b) At low temperatures only the magnons with low energy are excited. We replace $\eta_{k'}$ by $\exp(-\hbar\omega_{k'}/kT)$, and $(1+\eta_k)$ by 1. (c) Approximating the magnon dispersion by

$$\omega_k = \omega_0 + Dk^2 + Ek^4$$

and using the results of Yelon and Vettier, one finds $D/a^2 = 4J_1 + 12J_2 \approx -0.12\ \text{cm}^{-1}$, and $E/a^4 = -\frac{1}{3}J_1 + 3J_2 \approx 1.71\ \text{cm}^{-1}$, where J_1 and J_2 are the host intraplane exchange constants. Thus the dispersion is extremely flat near $k\approx 0$, and has a small negative initial curvature, which may not be of any practical significance. We approximate the dispersion by $\omega_k = \omega_0 + Ek^4$. Note that the $k=0$ frequency is

$$\omega_0 = \omega_g \pm g_h\mu_B H_0/\hbar, \tag{12}$$

where the two signs refer to the two sublattices, ω_g is the gap frequency and g_h is the host g value. (d) At low temperatures the upper limits of the integrals can be extended to infinity. Evaluation of Eq. (11) thus leads to

$$W_+(-\tfrac{5}{2}\to-\tfrac{3}{2}) = \frac{5}{16\hbar}\left(\frac{E}{a^4}\right)^{-3/2}(g_i g_h \mu_B^2)^2 \times\left(\sum_i{}' 3\sin\theta_i\cos\theta_i r_{iy}/r_i^3 a\right)^2 \times\exp(-\hbar\omega_0/kT)I(\omega_e, T), \tag{13a}$$

where

$$\frac{I(\omega_e,T)}{(\omega_e)^{1/2}} = \left(\frac{\pi kT}{\hbar\omega_e}\right)^{1/2}\left\{1+\exp\left(\frac{-\hbar\omega_e}{kT}\right) - \text{erf}\left[\left(\frac{\hbar\omega_e}{kT}\right)^{1/2}\right]\right\} \tag{13b}$$

is of the order of unity. The sum $|\sum'|^2$ was evaluated by computer by summing over rectangular shells of spins, and is found to converge extremely slowly, reaching $\frac{1}{4}$ of its final value at the fifth shell (including 60 neighbors), and $\frac{1}{2}$ its final value of the tenth shell (including 220 neighbors). Since the linear expansion of $\sin(\vec{k}-\vec{k}')\cdot\vec{r}_i$ breaks down at very low $\vec{k}-\vec{k}'$ for more distant shells, giving way to oscillatory behavior, we arbitrarily cut off the sum $\sum'$ at the fifth shell. This cutoff gives a reasonable agreement with the data.

In Fig. 4 we show the nuclear linewidths predicted by Eqs. (11), (12), and (13):

$$\frac{1}{T_{2n}}(b\colon -\tfrac{5}{2}) = W_+ ,$$
$$\frac{1}{T_{2n}}(b\colon +\tfrac{5}{2}) = W_- = W_+\exp(+\hbar\omega_e/kT), \tag{14}$$
$$\frac{1}{T_{2n}}(a\colon -\tfrac{5}{2}) = W_+ ,$$

together with the corresponding data.

In order to fit the data we used the measured values (YV) for the spin-wave gap $\omega_0 = 17.3\ \text{cm}^{-1}$, and $g_h = 3.5$. We also assigned the positive sign in the frequency Eq. (12) to b-sublattice impurities (a-sublattice host) to fit the slope and magnitude of the data. Note that none of the previous measurements was capable of determining this sign.

This determination identifies the a sublattice with host spins down, giving $H_d = -8000$ Oe. Together with $H_{\text{int}} = +2800$ Oe, we are able to distinguish between the two possible values of intra- and interplane exchange constants $J'_{\alpha\alpha}$ and $J'_{\alpha\beta}$ of MCM. We find the first possibility to be the correct one, with

$$J'_{\alpha\alpha} = -5650\ \text{Oe}, \quad J'_{\alpha\beta} = -8850\ \text{Oe},$$

by using the value $-14\,500$ Oe from the note on new

experimental data of MCM. We can also use the sublattice identification to choose between the two possible values of H_{ST}. We find that

$$H_{ST} = +11.31 \text{ kOe}.$$

Since H_{ST} may have contributions from more than one type of host Fe^{2+} spin, we have not converted it to an interaction strength.

Not all the features of the linewidth are understood. While the same coefficient and of course the same gap and g factors fit Eq. (14) quite well to the data of the lines corresponding to $M_s = \pm\frac{5}{2}$ for sublattice b, the same is not true for the data for sublattice a shown in Fig. 4. As a result of the decreasing magnon frequency with increasing field for sublattice a, one does expect larger relaxation rates for this sublattice, as observed. However, only with a magnitude nearly 3 times as large as the one for the b sublattice can the result of Eq. (14) explain the data for a.

The reason for the diagreement is not understood, although many approximations have been made which might lead to such errors. If the off-diagonal exchange J^{yz} were included, it would be added to the dipolar D^{yz} inside the sum $\sum'$ over neighbor spins. It could thus either increase or decrease the overall rates, depending on the relative signs of J^{yz} and D^{yz}. It is reasonable to assume, however, that since D^{yz} alone accounts fairly well for the observed rates, that the effect of J^{yz} is certainly not much larger than D^{yz}, and is probably smaller. Thus we are able to place a rough upper bound on J^{yz} of ≈ 0.04 cm^{-1}.

One should also notice that if the contribution of the off-diagonal exchange is important, our identification of the a sublattice with host spin down is questionable. Unlike the dipolar interaction, off-diagonal exchange between spins within the planes is not forbidden, so that relaxation through these interactions could involve magnon scattering on the same sublattice. This would change the identification of the sublattice-spin assignment, as well as the intra and interplane exchange constants and the supertransferred hyperfine interaction. So long as the whole set of linewidths is not completely understood, the identification of these parameters cannot be considered completely reliable.

The approximations that $\omega_k = \omega_0 + Ek^4$ within the planes, that spin waves are entirely localized on one sublattice or the other, and the low-k approximation to the dipolar sum are possible sources of the above-mentioned disagreement. However, all the effects we have observed are in the direction of reducing the difference between the a- and b-sublattice rates, rather than increasing it, as required to fit the data.

V. LINEWIDTH AND RELAXATION OF THE EPR

Although no extensive linewidth measurements of the impurity electronic resonance were made by MCM, the lines were observed to broaden and disappear at a temperature of roughly 8 K. We estimate that the linewidths required must have been at least 200 Oe. The electronic relaxation rate $1/T_{1e} = 2W_+/[S(S+1) - M_s M_s']$ was inferred from the nuclear relaxation, and extrapolated to $T \sim 8$ K, and is roughly two orders of magnitude too small to account for this observation. Therefore, we have attempted to calculate the electronic transverse relaxation rate due to a similar two-host-magnon scattering process via the isotropic impurity-host exchange J',

$$\frac{1}{T_{2e}} \sim \frac{4\pi}{\hbar^2}\left(\frac{ZJ'}{N}\right)^2 \sum_{kk'} (\eta_{k'} + 1)\eta_k \gamma_{k-k'} \delta(\omega_k - \omega_{k'}). \quad (15)$$

Here $\gamma_{k-k'} = \cos^2\frac{1}{2}(\vec{k} - \vec{k}') \cdot (\vec{r}_i - \vec{r}_{i'}) \sim 1$ for small k, and $|\vec{r}_i - \vec{r}_i'|$ is the nearest-neighbor distance a. Replacing the sum by integrals and assuming

$$\omega = \omega_0 + Ek^4,$$

we find

$$\frac{1}{T_{2e}} \sim \frac{(ZJ')^2}{16\hbar\pi E/a^4} e^{-\hbar\omega_0/kT} \int_0^\infty \frac{d\omega}{\omega} e^{-\hbar\omega/kT} \quad (16)$$

with a roughly logarithmic divergence, due to a combination of the flatness of the dispersion (Ek^4) and the large density of states at low k in two dimensions. If the small negative term Dk^2 is added to the dispersion, the divergence is moved away from $k = 0$ and made much stronger, which implies a breakdown in the perturbation approach used in the magnon scattering calculation. Nevertheless, other effects, such as finite magnon widths, would limit the divergence. It appears that not nearly enough is known about the system to allow an accurate prediction of $1/T_{2e}$. However, it is clear that the exponential form of Eq. (16) would adequately fit the data, while the divergent term could easily account for a numerical factor of 10^2.

VI. CONCLUSION

We have observed the NMR of the impurity ^{55}Mn nucleus in metamagnetic $FeBr_2$ at low temperatures. Due to the presence of the low-lying electronic mode spectrum of the Mn^{2+} electronic spin, the nuclear spectrum shows strong mixing with the

electronic one, giving effects such as nonlinear field-dependent frequencies and strong enhancements. The electronic relaxation times are found to be so long below 4 K that nuclear resonance is done while in fixed levels of M_s, giving several sets of spectra corresponding to different values of M_s. The temperature dependence of the electronic T_{1e} gives a lifetime broadening $1/T_{2n}$ of the nuclear resonance, which broadens and disappears above 4 K. The electronic relaxation $1/T_{1e}$ is explained by a two-magnon scattering process via the off-diagonal dipolar interaction D^{yz}. The unusually large magnitude of the process is due to the nearly two-dimensional nature of the magnetic excitations, as well as their extremely flat dispersion at low k.

ACKNOWLEDGMENTS

The authors gratefully acknowledge the support of Professor V. Jaccarino, and his many helpful discussions concerning the interpretations of these experiments. We also wish to thank S. Legrand of Saclay for the preparation of the single crystal used in the experiment. This work was supported in part by the National Science Foundation Grants No. GF42494 and DMR75-03847, and partly by Financiadora de Estudos e Projectos (FINEP), Conselho Nacional de Desenvolvimento Científico e Tecnológico (CNPq), and Comissão de Aperfeicoamento de Pessoal de Nível Superior (CAPES) (Brazilian Agencies).

[1]An extensive review and numerous references are given by R. A. Cowley and W. J. L. Buyers, Rev. Mod. Phys. 44, 406 (1972).
[2]T. Ishikawa, J. Phys. Soc. Jpn. 35, 434 (1973).
[3]W. B. Yelon and C. Vettier, J. Phys. C 8, 2760 (1976).
[4]A. R. Fert, P. Carrara, M. C. Lanusse, G. Mischler, and J. P. Redoules, J. Phys. Chem. Solids 34, 223 (1973).
[5]A. R. Fert, J. Leotin, J. C. Ousset, D. Bertrand, P. Carrara, and S. Askenazy, Solid State Commun. 18, 327 (1976).
[6]G. Mischler, P. Carrara, and Y. Merle D'Aubigné, Phys. Rev. B 15, 1568 (1977).
[7]H. Nishihara, J. Phys. Soc. Jpn. 43, 831 (1977).
[8]M. Date and M. Motakawa, Phys. Rev. Lett. 15, 855 (1965).
[9]N. Fujii, M. Motakawa, and M. Date, J. Phys. Soc. Jpn. 25, 700 (1968).
[10]Nai Li Huang, R. Orbach, E. Simánek, J. Owen, and D. R. Taylor, Phys. Rev. 156, 383 (1967).
[11]D. Hone, H. Callen, and L. R. Walker, Phys. Rev. 144, 283 (1966).
[12]M. Butler, V. Jaccarino, N. Kaplan, and H. J. Guggenheim, Phys. Rev. B 1, 3058 (1970).
[13]G. L. McPherson, R. C. Koch, and G. D. Stucky, J. Chem. Phys. 60, 1424 (1974).
[14]A. Abragam, *The Principles of Nuclear Magnetic Resonance* (Oxford U.P., Oxford, England, 1961), Chap. 6, p. 194.
[15]B. Bleaney, A. H. Cooke, F. N. H. Robinson, and M. R. Wells, Physica 86-88B, 1145 (1977).
[16]D. Beeman and P. Pincus, Phys. Rev. 166, 359 (1968).
[17]M. Tachiki, J. Phys. Soc. Jpn. 25, 686 (1968).